International Journal of Mechanical Engineering and Technology (IJMET)
Volume 9, Issue 3, March 2018, pp. 475–483, Article ID: IJMET_09_03_048
Available online at http://www.iaeme.com/ijmet/issues.asp?JType=IJMET&VType=9&IType=3
ISSN Print: 0976-6340 and ISSN Online: 0976-6359

EFFECT OF VOLUMETRIC BLOCKAGE RATIO ON THERMAL PLUME CHARACTERISTICS IN HORIZONTAL CHANNEL

D.Waman Waikar and R.Harish
School of Mechanical and Building Science, VIT, Vandalur-Kelambakkam Road, Chennai, India

ABSTRACT

In the present study we investigate the buoyancy induced turbulent flow characteristics in a ceiling ventilated horizontal channel with an internal heat source. Numerical analysis is performed in the channel for two different Grashof number Gr=7.88 x 10^{11} and 1.18 x 10^{12} and the volumetric blockage ratio is varied from 0.012 to 0.055. It is found that by increasing the Grashof number to Gr=1.18 x 10^{12}, the net mass flow rate through the central, upstream and downstream vents are increased by 23%, 16% and 15% respectively. It is also identified that by increasing the volumetric blockage ratio, the average temperature for Gr=7.88 x 10^{11} and 1.18 x 10^{12} are increased by 26.4% and 38.6%; while the average longitudinal velocity are decreased by 56% and 44% respectively.

Keywords: Grashof number, Horizontal vent, Volume Blockage Ratio

Cite this Article: D.Waman Waikar and R.Harish, Effect of Volumetric Blockage Ratio on Thermal Plume Characteristics in Horizontal Channel, International Journal of Mechanical Engineering and Technology, 9(3), 2018, pp. 475–483.
http://www.iaeme.com/IJMET/issues.asp?JType=IJMET&VType=9&IType=3

1. INTRODUCTION

In the event of fire accidents in rail and road tunnels, ventilation plays a crucial role in removing the smoke and hot gases trapped inside the tunnel. The buoyant gas that arises from the heat source propagates in the longitudinal direction and increases the temperature inside the tunnel. Hence ventilation [1-2] is of great significance in removing the hazardous gases and in reducing the tunnel temperature.

The important parameters in the study of tunnel ventilation are the maximum temperature [3], critical velocity [4-5], smoke back-layering flow length [4-6], temperature decay [7] and smoke removal efficiency [8]. Li et al. [3] identified that the maximum gas temperature beneath the tunnel ceiling increases linearly with the heat release rate and decreases linearly with the longitudinal ventilation velocity. Further experimental and theoretical studies were performed by Li et al.[4] to investigate the critical velocity together with back layering length

in tunnels. They found the critical Froude number and Richardson number and also proposed a co-relation based on the experimental data to predict the back layering length. Similar studies [5-8] were performed to identify the effect of ventilation velocity on the temperature and smoke layering length.

Harish and Venkatasubbaiah [9] investigated the effects of natural roof ventilation on the tunnel fire flow characteristics. They performed various parametric studies by varying the number of vents, heat source strength, location and varying the spacing between vents. Lee and Tsai [10] studied the effect of vehicular blockage in longitudinal ventilated tunnel for different ventilation velocities and identified the critical ventilation velocity. They found that critical ventilation velocity decreased in the absence of blockage upstream of the heat source. Gannouni [11] investigated the effects of vehicular obstacles on fire plumes by varying the relative position of the vehicles from the tunnel floor and the longitudinal ventilation velocity. They found that critical ventilation velocity decreased in the presence of vehicular obstacles when compared to empty tunnel. They also found that back layering length of smoke is less in the tunnel with obstacles than in empty tunnel [11]. Wang et al [12], studied the tunnel flame characteristics by changing the geometrical shapes of the heat source. They found that the geometrical shape of the heat source significantly affects the flame propagation. However, in the presence of large obstacle downstream of the heat source, the effect of heat source geometry was insignificant. Alva et al [13] conducted small scale experiments to investigate the effect of vehicular blockage in the tunnel. They found that due to vehicular obstacles the critical ventilation velocity reduces as a function of blockage ratio. They also found that relative size of vehicular obstacle and distance from the heat source significantly affects the critical ventilation velocity and smoke back layering length.

In the literature, various investigations were performed on thermal plume characteristics in forced ventilated tunnel with different ventilation velocities. However, studies on thermal plume characteristics in naturally ventilated tunnel in the presence of obstacles are very limited. This has been the motivation for the present study. In the present study investigations are performed in a naturally ventilated tunnel with three roof openings in the presence of vehicular obstacles. The parametric study is performed by varying the strength of the heat source, the location and shape of the obstacles.

2. MODELLING AND NUMERICAL METHODS

The horizontal channel considered in the present study is of 10 m long, 0.3 m wide and 0.25 m high. The heat source is of 1 m long and 0.1 m wide and is centrally located in the bottom wall of the channel. The tunnel top boundary consists of three vents; upstream vent, central and downstream vent each of dimensions 0.1 m wide and 0.5 m long located at one third, middle and two third centrally along the length of the channel. Figure 1 shows the front view of the channel with two vehicular obstacles each of 0.5 m long, 0.1524 m wide and 0.1524 m high placed exactly at upstream and downstream of the heat source.

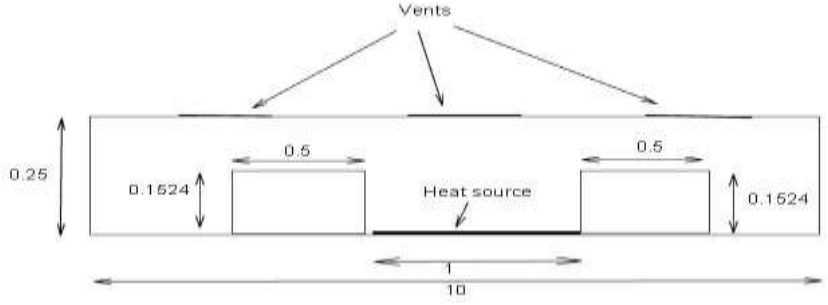

Figure 1 Schematic diagram of channel: Front view (all dimensions are in m)

The volume blockage ratio is denoted by symbol δ and is defined as the ratio of total volume of vehicular blockages to the total volume of the horizontal channel. The volume blockage ratio for the case shown in figure 1 is δ = 0.012192. Figure 2 shows the different arrangement of vehicular obstructions considered in the present study with different volume blockage ratio. In figure 2, case A indicates two obstacles which are placed side by side on the upstream side of the heat source with a blockage ratio of 0.012192.

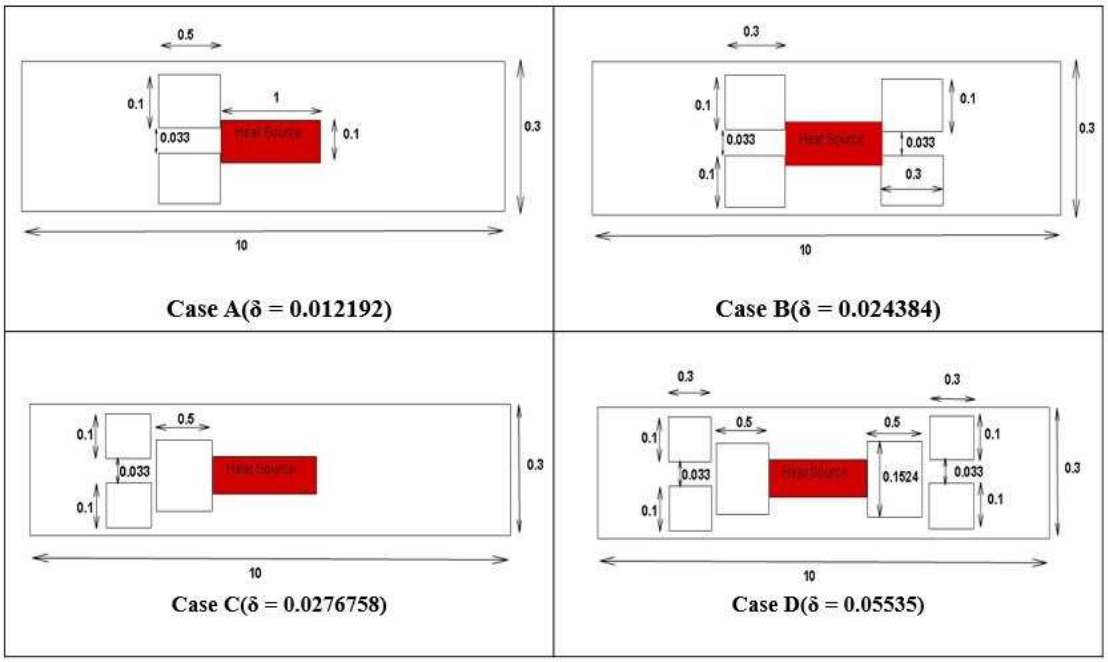

Figure 2 Top view of the channel with various arrangements of obstacles (all dimensions are in m)

In case B, four vehicular obstacles each of 0.3 m long, 0.1 m wide and 0.1524 m high are placed side by side at the upstream and downstream side of the heat source. The corresponding volume blockage ratio is δ = 0.024384. In case C, we have three obstacles located at the upstream side of the heat source. The first obstacle located close to the heat source is of 0.5 m long, 0.1524 m wide and 0.1524 m. The second and third obstacles are of smaller size and placed side by side behind the first obstacle as shown in figure 2, case c. The corresponding δ value is 0.027658. Case D indicates the arrangement with six vehicular obstructions placed at both sides of the heat source with δ value of 0.05535. The strength of the heat source is denoted by a dimensionless number called Grashof number (Gr). The Grashof number is the ratio of the buoyancy force to viscous force.

The Grashof number is mathematically represented as follows: $Gr = \frac{g\beta\Delta TL^3}{\upsilon^2}$; where 'g' indicates gravity, 'β' is co-efficient of thermal expansion of air, 'ΔT' is the temperature difference between the heat source and ambient air, 'L' is the length of the horizontal channel and 'ν' indicates the kinematic viscosity of air. The investigations are performed for two different Grashof numbers Gr = 7.88 x 10^{11} and 1.18 x 10^{12} with corresponding temperature differences of ΔT= 600 K and 900 K respectively.

The numerical simulations are performed by using Ansys Fluent 16.0 a Finite Volume Solver (FVM), where the problem is modeled as buoyancy induced turbulent flows. The turbulent flow problem is modeled by solving the Reynolds Averaged Navier-Stokes (RANS) equation for the velocity fields along with the time averaged energy equation for the temperature field. The turbulence is modeled by the realizable k- ε turbulence model for the

kinetic energy and dissipation rate. The radiation effects are included by using the surface to surface radiation model. The pressure velocity coupling is avoided by using SIMPLE algorithm and the convergence criterion is set to a small time step of 10^{-5}. The ambient temperature inside the tunnel is set at 300 k and temperature difference between the heat source and ambient temperature is maintained according to the Grashof number. The material properties of concrete are specified to the inside linings of the tunnel. Open boundary conditions are specified at tunnel entrance, tunnel exit and along the roof vents. Due to this boundary condition, we can take into account the bidirectional exchange of the ambient cold and hot fluid inside the tunnel. The temperature of fluid leaving the channel satisfies the upwind boundary condition. No slip boundary condition is specified on the channel walls for the velocity fields. The buoyancy effects are modeled using Boussinesq approximation which is widely used when the density changes are small and it also reduces the non-linearity of the problem.

3. VALIDATION

The capability of the present numerical model is validated with experimental results available in literature. Lee and Ryou [14] performed experimental study in longitudinal tunnels with different aspect ratios. We validate our numerical results with the experimental results for the cases where the tunnel is of aspect ratio 0.5 and 10.4 m long. Aspect ratio is defined as the ratio of height of the tunnel to its width. In this experiment [14] seven thermo couples were fitted below the ceiling towards the tunnel exit to measure the temperature distribution. The fire source intensity is of 8.27 kW and is kept at 3 m from the left opening. Figure 3 indicates the variation of temperature as we move away the heat source. It is evident that the temperature near the ceiling decreases as we move towards the tunnel exit. The same trend is also observed in our numerical simulations and from the plots it is observed that there is an excellent agreement between our numerical results with the experimental results available in literature.

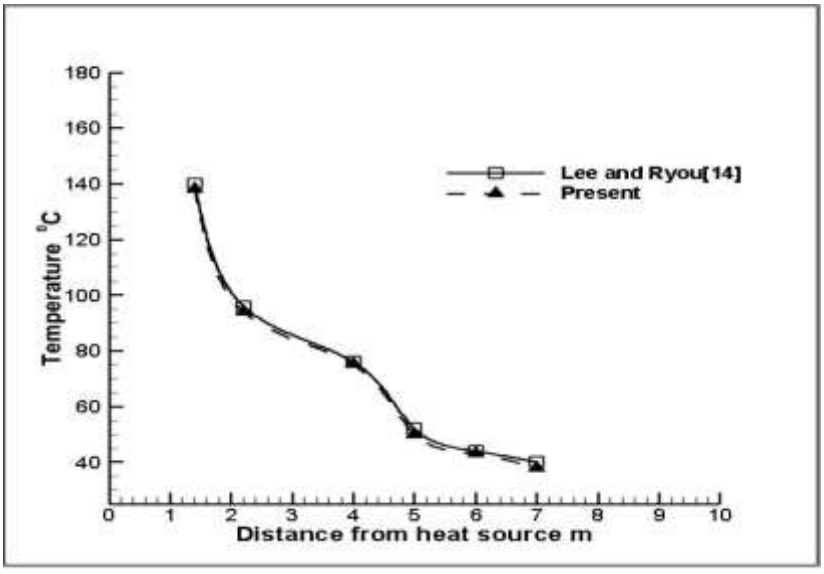

Figure 3 Validation with experimental results

4. RESULTS AND DISCUSSION

Figure 4 shows the iso-surface of thermal plume rising from the heat source and propagating towards the channel side boundaries. The analysis is performed for Gr=7.88 x 10^{11} with δ=0.012192.

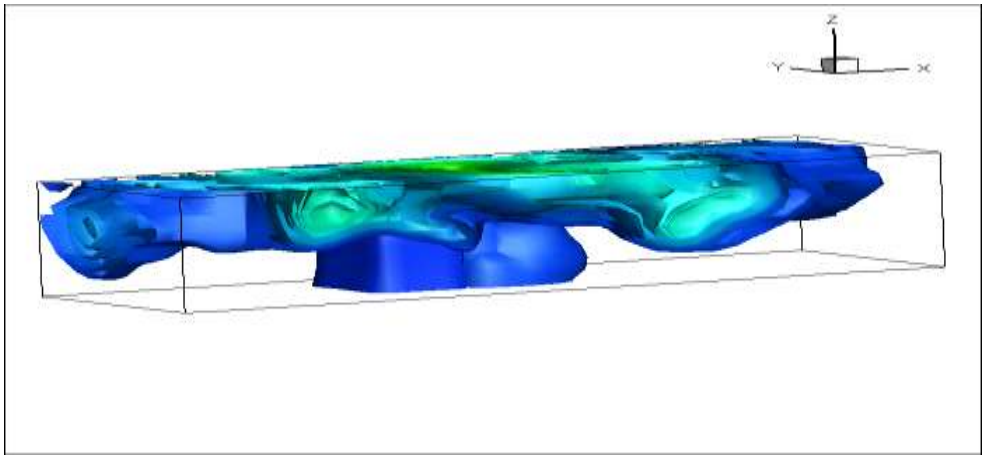

Figure 4 Iso-surface of thermal plumes

We can see that the buoyancy force strengthens the propagation of thermal plume and the vehicular obstruction placed closer to the heat source restricts the free flow of buoyant gas. The hot gas accumulates near the top surface of the channel and as flow progresses, the buoyant gases are seen settling towards the channel bottom surface. Figure 5 shows the temperature distribution inside the horizontal channel with vehicular obstruction. The maximum temperature is observed closer to the heat source and the heat diffuses as the plume spreads in the longitudinal direction towards the channel side boundaries. The region above the vehicular obstruction has a higher temperature of 98^{o} C as more heat gets accumulated in this region. The asymmetric temperature distribution shown in figure 4 clearly indicates that the vehicular blockage restricts the longitudinal movement of plume towards the channel left boundary.

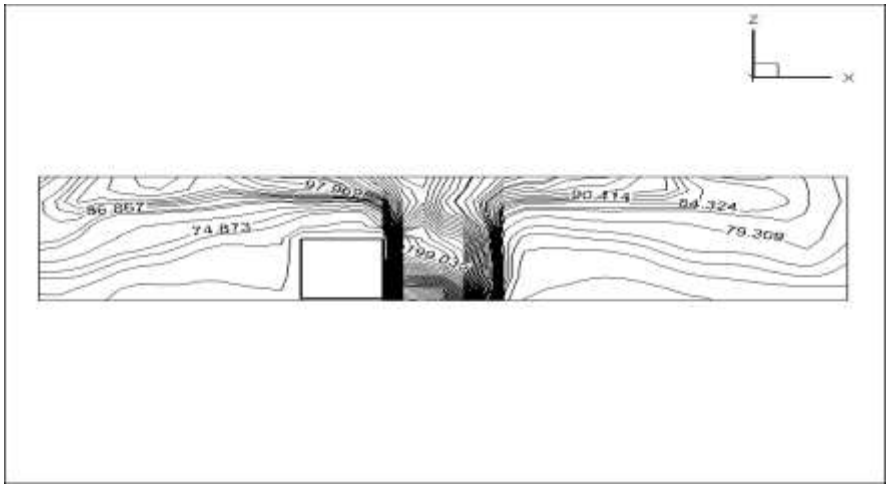

Figure 5 Variation of temperature contours along the length of tunnel in ^{0}c

Figure 6 shows the variation of mass flow rate with time across all the three vents located at the upstream, center and downstream side of the channel. It is evident from the plots that the net mass flow rate is significant through the central vent when compared to the upstream and downstream vent. Since the heat source is located above the central vent more amount of hot fluid leaves the channel through the centrally located vent. Since the channel considered in the present study is symmetric, the mass flow rate across the upstream and downstream vents shows a similar pattern. The flow across all the three vents are bidirectional and as the hot fluid leaves the channel; significant amount of ambient fluid entrains into the channel through the tunnel vent openings. Hence the oscillations observed in the mass flow rate plots

are due to the bidirectional exchange across the tunnel vent openings. In the present study it is identified that the flow rate through the central vent is 40% higher than the flow rate through the upstream and downstream vent. It is also observed that the difference in flow rates between the upstream and downstream vent is less than 3%.

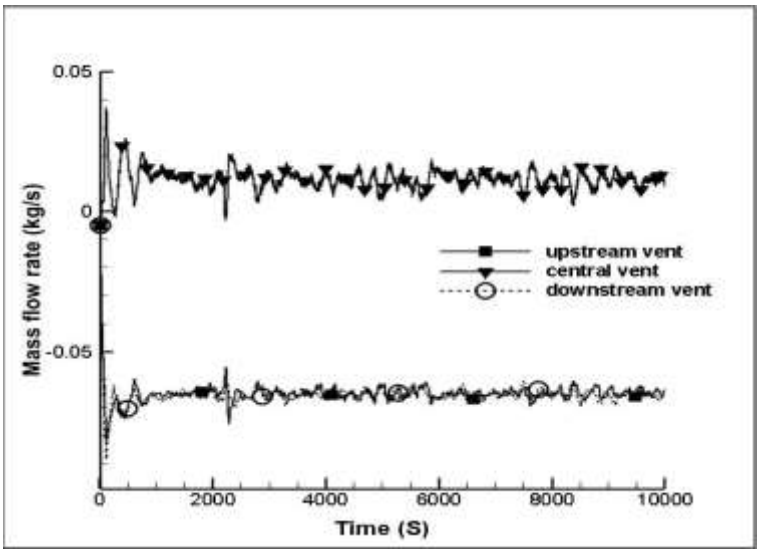

Figure 6 Variation of mass flow rate with time

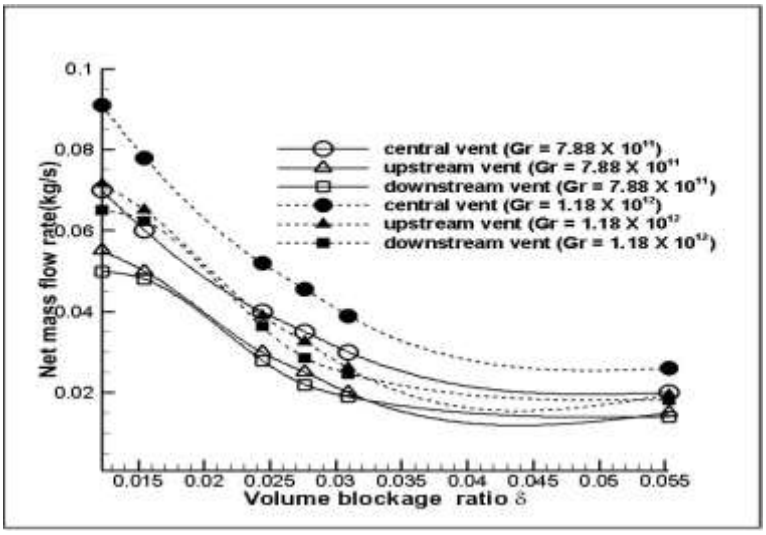

Figure 7 Variation of net mass flow rate with volume blockage ratio (δ)

Figure 7 shows the comparison of net mass flow rate with different volume blockage ratio for two different Grashof number Gr = 7.88 x 10^{11} and 1.18 x 10^{12}. From figure 7, it is evident that with increase in volume blockage ratio the net mass flow rate decreases across all the three vents. As the volume blockage ratio (δ) is increased, the number of obstructions placed inside the channel increases and it opposes the spreading of thermal plume inside the horizontal channel. Hence the net mass flow rate decreases with increase in volume blockage ratio (δ). It is also seen that the net quantity of fluid leaving the horizontal channel through the central vent is higher than the upstream and downstream vent. A comparison is also shown between two Gr values. It is observed that with increase in Grashof number the strength of the heat source increases and more amount of hot fluid leaves the horizontal channel through the vents. The buoyancy force developed from Gr=1.18 x 10^{12} is higher than Gr=7.88 x 10^{11} and the higher buoyancy force assists the propagation of thermal plume. Hence the net mass flow

rate plotted across all the three vents are higher for Gr=1.18 x 10^{12} in comparison with Gr=7.88 x 10^{11}. For Gr=1.18 x 10^{12}, the net mass flow rate through the central, upstream and downstream vents are increased by 23%, 16% and 15% respectively.

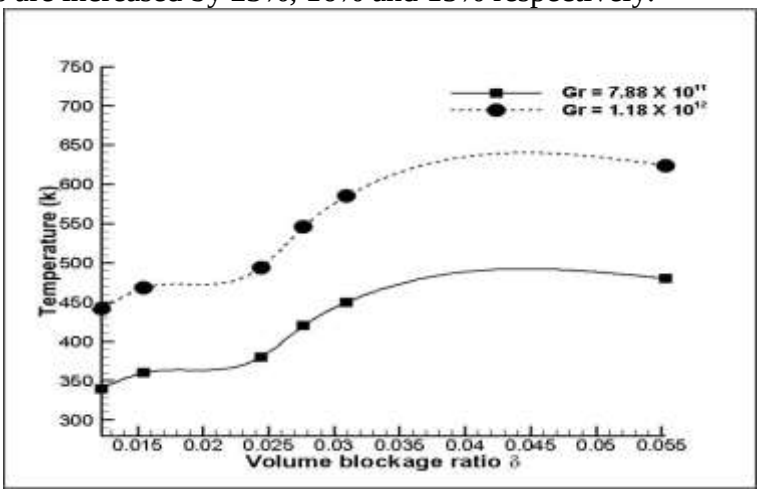

Figure 8 Variation of average temperature with volume blockage ratio δ

Figure 8 indicates the variation of average temperature measured at a height of 0.18m longitudinally throughout the entire length of the channel. It is evident that with increase in volume blockage ratio the average temperature inside the tunnel increases. It is also observed that for a lower value of δ=0.012, Gr=7.88 x 10^{11}, the average temperature is 340 K and by increasing δ=0.055, the peak temperature rises is 430 K. For Gr=7.88 x 10^{11} with increase in volume blockage ratio, the average temperature inside the horizontal channel is increased by 26.4%. For Gr=1.18 x 10^{12} and δ=0.012 the average temperature measured inside the channel is 440 K; however with increase in δ=0.055 the peak temperature reached is 610 K. For Gr=1.18 x 10^{12} with increase in volume blockage ratio, the average temperature inside the horizontal channel is increased by 38.6%. Moreover, with rise in Grashof number the average temperature inside the tunnel is increased by 36%.

Figure 9 indicates the variation of average longitudinal velocity of thermal plume measured across the entire length of the horizontal channel at a height of 0.18m. It is evident from the plots that the average longitudinal velocity decreases with increase in volume blockage ratio (δ). As δ increases, significant amount of hot gases are trapped inside the horizontal channel and the vehicular blockage also obstructs the plume longitudinal movement. This results in a lower average longitudinal velocity inside the channel.

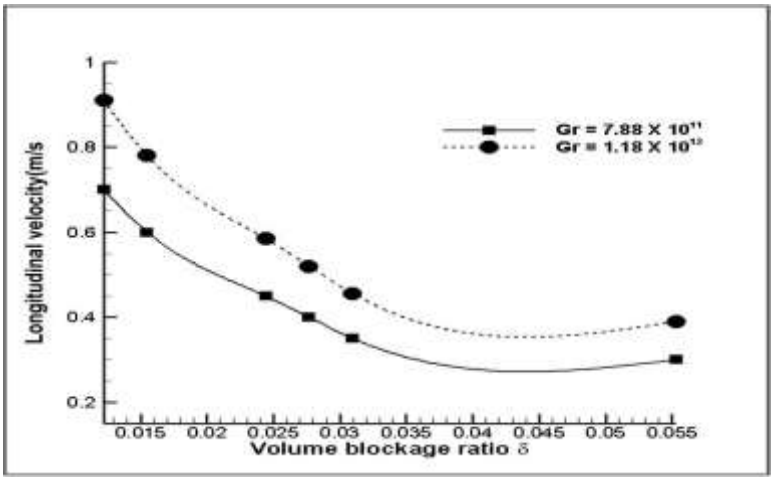

Figure 9 Variation of average longitudinal velocity with volume blockage ratio (δ)

For δ=0.012 and Gr=7.88 x 10^{11}, the average longitudinal velocity measured is 0.7 m/s and with increase in δ=0.055, the longitudinal velocity is reduced to 0.3m/s. For Gr=7.88 x 10^{11} by increasing the volume blockage ratio, the average longitudinal velocity inside the horizontal channel is reduced by 56%. For Gr=1.18 x 10^{12} and δ=0.012 the average longitudinal velocity measured inside the channel is 0.9 m/s; however with increase in δ=0.055 the longitudinal velocity is reduced to 0.5 m/s. For Gr=1.18 x 10^{12} with increase in volume blockage ratio, the average longitudinal velocity inside the horizontal channel is reduced by 44%. Moreover, with rise in Grashof number the average longitudinal velocity inside the tunnel is reduced by 22%.

5. CONCLUSION

In the present work, we investigate the effects of volumetric blockage ratio on thermal plume behavior in ventilated channel. The horizontal channel consists of three vents and an internal heat source. Analysis is performed for two different Grashof number Gr=7.88 x 10^{11} and 1.18 x 10^{12} and the volumetric blockage ratio is varied from 0.012 to 0.055. In the present study, it is identified that the flow rate through the central vent is 40% higher than the flow rate through the upstream and downstream vent. Moreover by increasing the Gr value to 1.18 x 10^{12}, the net mass flow rate through central, upstream and downstream vents are increased by 23%, 16% and 15% respectively. It is also observed that for δ=0.012 and Gr=7.88 x 10^{11}, the average temperature reached is 340 K and by further increasing δ=0.055, the average temperature is increased to 430 K. It is also identified that by increasing the volumetric blockage ratio, the average temperature for Gr=7.88 x 10^{11} and 1.18 x 10^{12} are increased by 26.4% and 38.6%; while the average longitudinal velocity are decreased by 56% and 44% respectively.

REFERENCES

[1] Nilsen, A.R., Log, T. Results from three models compared to full-scale tunnel fires tests. Fire safety Journal, 44, 2009, pp.33-49.

[2] Beard, A., Carvel, R. The Handbook of Tunnel Fire Safety. Thomas Telford Publisher, 2012.

[3] Li, Y.Z., Lei, B., Ingason, H. The maximum temperature of buoyancy-driven smoke flow beneath the ceiling in tunnel fires. Fire safety Journal, 46, 2011, pp. 204-210.

[4] Li, Y.Z., Lei, B., Ingason, H. Study of critical velocity and back layering length in longitudinally ventilated tunnel fires. Fire safety Journal, 45, 2010, pp.361-370.

[5] Weng, M.C., Lu, X.L., Liu, F., Du, C.X. Study on the critical velocity in a sloping tunnel fire under longitudinal ventilation. Applied Thermal Engineering, 94, 2016, pp.422-434.

[6] Hu, L.H., Huo, R., Chow, W.K. Studies on buoyancy-driven back-layering in tunnel fires. Experimental Thermal and Fluid Science, 32, 2008, pp.1468-1483.

[7] Wang, Y.F., Qin, T., Sun, X.F., Liu, S., Jiang, J.C. Full-scale fire experiments and simulation of tunnel with vertical shafts. Applied Thermal Engineering, 105, 2016, pp.243-255.

[8] Wang, Y., Jiang, J., Zhu, D. Full-scale experiment research and theoretical study for fires in tunnels with roof openings. Fire Safety Journal, 44, 2009, pp.339-348.

[9] Harish, R., Venkatasubbaiah, K. Effects of buoyancy induced roof ventilation systems for smoke removal in tunnel fires. Tunneling and Underground Space Technology, 42, 2014, pp.195-205.

[10] Lee, Y.P., Tsai, K.C. Effect of vehicular blockage on critical ventilation velocity and tunnel fire behavior in longitudinally ventilated tunnels. Fire Safety Journal, 53, 2012, pp.35-42.

[11] Gannouni, S., Maad, R.B. Numerical study of the effect of blockage on critical velocity and backlayering length in longitudinally ventilated tunnel fires. Tunnelling and Underground Space Technology, 48, 2015, pp.147-155.

[12] Wang, X., Fleischmann, C., Spearpoint, M. Assessing the influence of fuel geometrical shape on fire dynamics simulator (FDS) predictions for a large-scale heavy goods vehicle tunnel fire experiment. Case Studies in Fire Safety, 5, 2016, pp.34-41.

[13] Alva, W.U.R., Jomaas, G., Dederichs, A.S. The influence of vehicular obstacles on longitudinal ventilation control in tunnel fires. Fire Safety Journal, 87, 2017, pp.25-36.

[14] Lee, S.R., Ryou, H.S. An experimental study of the effect of the aspect ratio on the critical velocity in longitudinal ventilation tunnel fires. Journal of Fire Science, 23, pp.119-138. 2005

[15] S Girish, M Surya Prakash, P Geeta Krishna and K Lavanya. Analysis of a Condenser in a Thermal Power Plant for Possible Augmentation in its Heat Transfer Performance. International Journal of Civil Engineering and Technology, 8(7), 2017, pp. 410–420.

[16] Surana Samyak, TP Manoj and Santhi A.S, A Parametric Study of Integral Bridges Subjected To Thermal Loading. International Journal of Civil Engineering and Technology, 8(4), 2017, pp. 431–440.